Lawrence Berkeley National Laboratory
LBL Publications

Title

Anthropogenic Contributions to the 2021 Pacific Northwest Heatwave

Permalink

https://escholarship.org/uc/item/7v61s1tg

Journal

Geophysical Research Letters, 49(23)

ISSN

0094-8276

Authors

Bercos-Hickey, Emily

O'Brien, Travis A

Wehner, Michael F

et al.

Publication Date

2022-12-16

DOI

10.1029/2022gl099396

Copyright Information

Peer reviewed

AGU
ADVANCING EARTH AND SPACE SCIENCE

Geophysical Research Letters®

Key Points:
- The Pacific Northwest (PNW) heatwave was unprecedented in the observational record over a large area
- Statistical and global climate models fail to inform about human influence on the PNW heatwave, as it is a far outlier
- Hindcast attribution methods can provide limited and conditional information about the human influence on the PNW heatwave

Correspondence to:

M. F. Wehner,
mfwehner@lbl.gov

Author Contributions:

Conceptualization: Emily Bercos-Hickey
Data curation: Emily Bercos-Hickey, Travis A. O'Brien
Formal analysis: Emily Bercos-Hickey, Michael F. Wehner
Investigation: Travis A. O'Brien, Michael F. Wehner, Likun Zhang, Mark D. Risser
Methodology: Michael F. Wehner, Christina M. Patricola
Visualization: Emily Bercos-Hickey, Likun Zhang
Writing – original draft: Emily Bercos-Hickey, Michael F. Wehner, Likun Zhang

Anthropogenic Contributions to the 2021 Pacific Northwest Heatwave

Emily Bercos-Hickey[1] [iD], Travis A. O'Brien[1,2] [iD], Michael F. Wehner[3] [iD], Likun Zhang[1,4] [iD], Christina M. Patricola[1,5] [iD], Huanping Huang[1,6] [iD], and Mark D. Risser[1] [iD]

[1]Climate and Ecosystem Sciences Division, Lawrence Berkeley National Laboratory, Berkeley, CA, USA, [2]Department of Earth and Atmospheric Sciences, Indiana University Bloomington, Bloomington, IN, USA, [3]Applied Mathematics and Computational Research Division, Lawrence Berkeley National Laboratory, Berkeley, CA, USA, [4]Department of Statistics, University of Missouri, Columbia, MO, USA, [5]Department of Geological and Atmospheric Sciences, Iowa State University, Ames, IA, USA, [6]Department of Geography and Anthropology, Louisiana State University, Baton Rouge, LA, USA

Abstract Daily maximum temperatures during the 2021 heatwave in the Pacific Northwest United States and Canada shattered century old records. Multiple causal factors, including anthropogenic climate change, contributed to these high temperatures, challenging traditional methods of attributing human influence. We demonstrate that the observed 2021 daily maximum temperatures are far above the bounds of Generalized Extreme Value distributions fitted from historical data. Hence, confidence in Granger causal inference statements about the human influence on this heatwave is low. Alternatively, we present a more conditional hindcast attribution study using two regional models. We performed ensembles of simulations of the heatwave to investigate how the event would have changed if it had occurred without anthropogenic climate change and with future warming. We found that global warming caused a ∼0.8°C–1°C increase in heatwave temperatures. Future warming would lead to a ∼5°C increase in heatwave temperature by the end of the 21st century.

Plain Language Summary While it is clear that global warming causes heatwaves to be warmer, the unique meteorological conditions behind the 2021 Pacific Northwest heatwave tax our ability to make quantitative estimates of the human contribution. We discuss why there is low confidence in traditional estimates of the human contribution to this heatwave's temperatures and present an alternative, albeit more highly constrained estimate that human activities caused a ∼0.8°C–1°C increase in the observed daily maximum temperatures. Additional future warming would lead to a ∼5°C increase in the heatwave by the end of the 21st century.

1. Introduction

On 26–29 June 2021, an unprecedented heatwave affected the Pacific Northwest (PNW) of the United States and western Canada. Temperature records were shattered, with all-time highs of 116°F (47°C) in Portland, Oregon, 108°F (42°C) in Seattle, Washington, and 121°F (49°C) in Lytton, British Columbia (Di Liberto, 2021). Heatwaves, characterized by prolonged periods of excessive heat, can have dangerous impacts on human health, infrastructure, and the environment (Campbell et al., 2018; McEvoy et al., 2009; Perkins-Kirkpatrick & Alexander, 2013; Ruffault et al., 2020), and the PNW heatwave was no exception. Over 500 deaths were attributed to the heatwave (Popovich & Choi-Schagrin, 2021), and the environment and infrastructure throughout the affected region were strained and damaged, with crops ruined and roads buckled due to the excessively hot temperatures (Baker & Sergio, 2021). The devastating and large-scale impacts of the PNW heatwave were exacerbated by the lack of adaptability of a region unaccustomed to such extreme high temperatures, with the observational record suggesting that this was a highly anomalous event (Figure 1).

The meteorological conditions of the PNW heatwave were similar to previous deadly heatwaves in Europe and Russia (Black et al., 2004; Dole et al., 2011). These events are associated with atmospheric blocking patterns, which are known to cause extreme heatwaves (Horton et al., 2015; Miralles et al., 2014; Schaller et al., 2018) and are characterized by a persistent, quasi-stationary, and often anticyclonic obstruction of the usual zonal flow (Rex, 1950; Sumner, 1954; Woollings et al., 2018). During the PNW heatwave, the high pressure of an omega block was centered over Washington and British Columbia (Figure S1 in Supporting Information S1) leading to subsidence and a multi-day period of hot, dry weather throughout the region (Neal et al., 2022). Additionally, an anomalous warm-season atmospheric river (AR) made landfall over the Alaska panhandle in late June and

Writing – review & editing: Travis A. O'Brien, Christina M. Patricola, Huanping Huang, Mark D. Risser

injected a large amount of moisture into western Canada and the PNW. The accumulation of water vapor under the high pressure of the atmospheric blocking pattern may have formed a positive feedback loop that further enhanced the heatwave (Lin et al., 2022; Mo et al., 2022). These two weather patterns were also superimposed on dry soil conditions, as 50% of Washington state and 70% of Oregon were in severe drought conditions in June 2021 (droughtmonitor.uni.edu).

An anomalously large rate of new high temperature records is consistent with expectations from global warming (Meehl et al., 2016; Perkins-Kirkpatrick & Gibson, 2017; Power & Delage, 2019). Heatwaves have increased since the 1950s (Perkins, 2015), and this observed increase in the frequency, intensity, and duration of heatwaves has been attributed to anthropogenic climate change (Diffenbaugh & Ashfaq, 2010; Meehl & Tebaldi, 2004; Min et al., 2013; Perkins et al., 2012; Wehner et al., 2018; Wuebbles et al., 2014). The 2021 PNW heatwave shattered previous records in the region by up to 5°C. Large ensemble climate model simulations suggest that extreme temperature variability increases with warming and that the rate of record shattering events depends on global warming rate more so than the global warming level itself (Fischer et al., 2021). The Intergovernmental Panel on Climate Change Sixth Assessment Report found that many heatwaves around the world could be attributed to human influence (Seneviratne et al., 2021). Future warming will further increase the frequency, intensity, and duration of heat extremes (Vogel et al., 2020), with the potential for temperatures to often reach dangerous levels for human health and agriculture (Sun et al., 2019).

The World Weather Attribution initiative (WWA, https://www.worldweatherattribution.org/) performed analyses of the PNW heatwave within weeks of the event and made three rapid attribution statements, which were later published in the scientific literature (Philip et al., 2021). First, they stated that the observed temperatures recorded were "virtually impossible without human-caused climate change." Second, after estimating that the observed temperatures had a return period of approximately 1,000 years, they stated that such annual maximum daily maximum temperatures (TXx) "would have been at least 150 times rarer without human-induced climate change." Third, they went on to state that "this heatwave was about 2°C hotter than a 1 in 1,000-year heatwave that at the beginning of the industrial revolution would have been."

In this study, our objective is to revisit these rapid attribution statements and to advance our understanding of how climate change affected the PNW heatwave. In Section 2, we discuss the limitations of statistical models to estimate the rarity of the PNW heatwave. In Section 3, we describe our experimental design of dynamical model simulations of the PNW heatwave under past, present, and future climate conditions using two regional climate models. In Section 4, we discuss the resulting temperature changes from these simulations. Finally, we present our conclusions in Section 5.

2. Statistical Modeling

Figure 1a shows maximum daily maximum temperatures between 25 June and 4 July 2021 from a homogenized US version of the Global Historical Climatology Network (GHCN) station data (Rennie et al., 2019). Figure 1a reveals that most stations in this region had values greater than 45°C. Figure 1b compares the summertime (June–August [JJA]) TXx from all of the US stations within the WWA region (45–49°N and 123–119°W) over 1920–2020 to those from 25 June to 4 July 2021. Figure 1c shows JJA TXx averaged over all of the US stations in this region for each year. From Figures 1b and 1c, it is clear that the PNW heatwave was an outlier event compared to previous summertime maximum temperatures and will challenge statistical modeling.

Philip et al. (2021) found that the 2021 spatially averaged temperatures from the ERA5 reanalysis (Hersbach et al., 2020) exceeded the upper bound of an out of sample (not including 2021) non-stationary generalized extreme value (GEV) distribution fit to data from 1950 to 2020. They then took a practical approach while acknowledging the limitations and included the 2021 values, estimating that the current return period of the PNW heatwave was about 1,000 years. Comparing this return period to that obtained under preindustrial temperatures, they concluded that the probability of the PNW heatwave was increased by a factor of 390. Further analysis of climate model simulations and their expert judgment caused them to conclude that the probability of the observed temperature was increased by *at least* 150 as their final synthesis attribution statement.

We repeat this non-stationary GEV analysis on individual station data from 1950 to 2020 instead of averaging over the WWA study region. In each single-station analysis, we use a GEV distribution with a location parameter linearly dependent on a sum-total forcing variable for five well-mixed greenhouse gases to accommodate
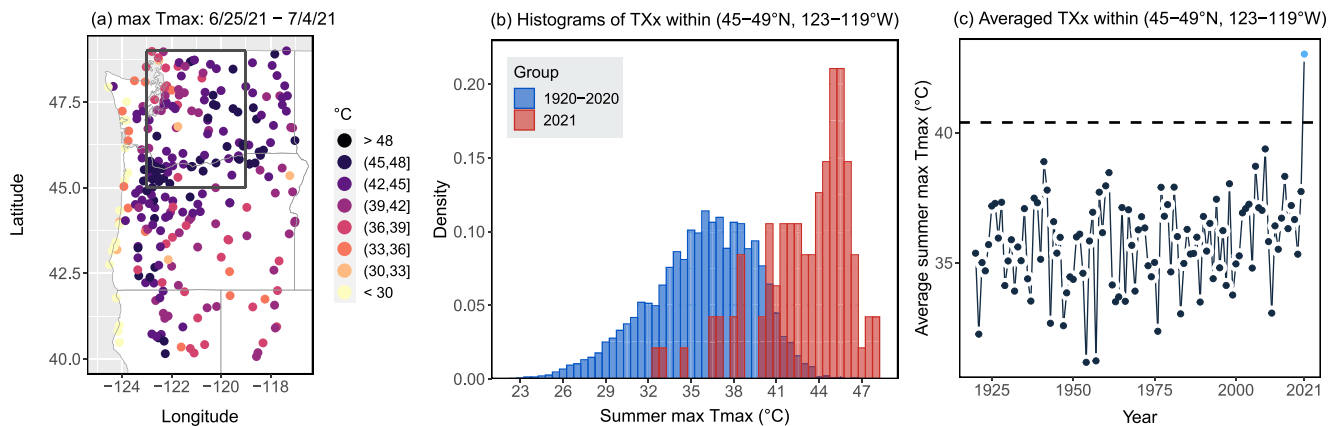
Figure 1. Observational station data from the homogenized US version of the Global Historical Climatology Network of (a) the maximum daily maximum temperature between 25 June and 4 July, (b) histograms of the summertime (June–August [JJA]) maximum daily maximum temperature (i.e., JJA TXx) from the US stations within the World Weather Attribution initiative (WWA) region (45–49°N and 123–119°W), as defined by Philip et al. (2021), in 1920–2020 and in 2021, and (c) the average JJA TXx by year from the US stations within the same region. The dashed line is the Bayesian expectation of the upper bound on daily maximum temperature averaged across the US stations within the region defined by the WWA.

non-stationarity (e.g., Risser et al. (2022)), which imposes a non-linear time trend in the GEV model (Section S1 in Supporting Information S1).

Figure 2a shows the Bayesian expectation of the upper bound for daily maximum temperatures for the 1950–2020 GHCN station data. Stations where the observed 2021 values exceed the expectation of the upper bound ("+") reveal that most of the heatwave's maximum temperatures are outside of the range of the GEV model. Figure 2b shows the 2021 out of sample return times for the GHCN stations, where many stations realized return times in excess of 2,000 years during the 2021 PNW heatwave. The probability of 2021 temperatures exceeding this GEV upper bound (Figure 2c) further illustrates that the out of sample GEV fails to describe the 2021 PNW heatwave. Including the 2021 temperatures in the GEV fitting procedure extends the upper bounds to include these values in the distribution, but the distributions are a poor fit to the rest of the data. Using a χ^2 goodness-of-fit test, the p-values calculated without 2021 values are generally greater than 0.2, demonstrating strong evidence of an underlying GEV distribution. However, the p-values calculated when 2021 temperatures are included are less than 0.05, indicating that the distribution is significantly different from GEV. Figure 1b, constructed by binning all GHCN station data from 1920 to 2020 (blue) and 2021 (red), further suggests that the temperatures of the 2021 heatwave are drawn from different distributions than previous years that is not accounted for by the
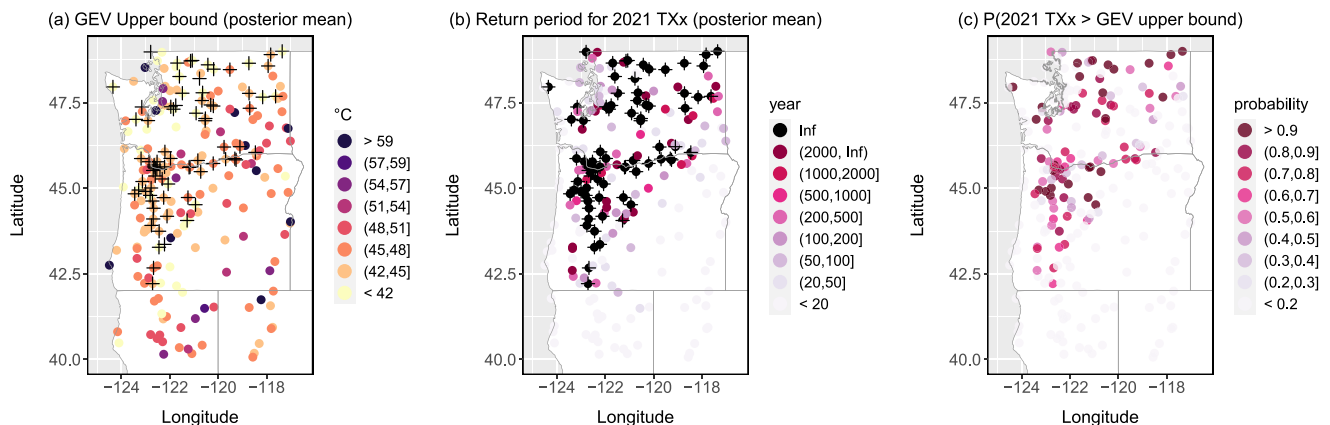
Figure 2. Results from fitting the non-stationary generalized extreme value (GEV) distribution to station data from 1950 to 2020: (a) Bayesian expectation (posterior mean) for the GEV distributional upper bound; (b) Bayesian expectation for the return periods of 2021 June–August (JJA) TXx (calculated using the fitted non-stationary GEV distribution). In both panels, "+" signifies that the 2021 JJA TXx exceeded the Bayesian expectation of the GEV distributional upper bound, which leads to infinite return periods in panel (b); and (c) The overall probability of 2021 TXx exceeding the GEV upper bound given the observations.

time-dependent greenhouse gas covariate. The above evidence suggest that the critical GEV assumption of independent and identically distributed (i.i.d.) data is violated when 2021 temperatures are included.

Given that an in-sample GEV distribution is a poor fit to the GHCN data and that the combined effects of the atmospheric blocking pattern and anomalous AR were likely very rare if not unique, we conclude that there should be little confidence in attribution statements based on in-sample GEV formulations. Philip et al. (2021) argued that the temperatures reached during the PNW heatwave were "virtually impossible" without climate change. However, this conclusion is not supported from a purely Granger causal inference perspective (Ebert-Uphoff & Deng, 2012; Hannart et al., 2016). Granger causality in this sense means that knowledge of greenhouse gas concentrations would inform about the probability of the 2021 heatwave temperatures. But due to the failure of the non-stationary GEV methodology to construct a well-fit in-sample distribution that includes the 2021 temperature values, and the fact that the out-of-sample distribution does not reach the magnitude of the 2021 event, no statement about the role of greenhouse gases should be made from this technique. The statistical analysis presented here only supports an attribution statement that these temperatures were virtually impossible under any previously experienced meteorological conditions, with or without global warming.

Given this evidence that the outlier 2021 temperatures are not drawn from the same distribution as all previous TXx values, we further conclude that TXx is not an appropriate attribution variable for this event. Hence, analysis of TXx from the CMIP global climate models is also inappropriate for understanding this event. Examination of the CMIP database for extreme temperatures of much greater rarity than TXx, either through longer block sizes or high thresholds provides a more sound basis to construct a distribution more suitable to describe events as rare as the PNW heatwave than do distributions of annual maxima. It is clear that ensemble sizes in the standard CMIP database are not large enough to construct such distributions and provide robust attribution statements. However, recent developments of larger climate model ensemble simulations (up to 40 individual realizations) do provide some insight as to the rarity of such events (McKinnon & Simpson, 2022).

Despite these limitations of conventional attribution methods, it is highly likely that anthropogenic climate change influenced the 2021 PNW heatwave. Hence, the next section describes a more constrained hindcast attribution method using short, high-resolution numerical weather prediction model simulations with initial and boundary conditions imposing the requisite large scale meteorological conditions which led to the 2021 PNW heatwave. By altering the anthropogenic factors, Pearl causal inference statements (Pearl, 2009) about only the change in magnitude of the PNW heatwave from global warming, can be informed by these constrained hindcasts models assuming a fixed but unspecified return time.

3. Dynamical Models and Experimental Design

From Section 2, the PNW heatwave of 2021 was an extreme outlier event. Traditionally, Pearl causal inference attribution statements are made with long simulations of global climate models, usually in pairs forced with both anthropogenic and natural forcing factors (Stott et al., 2016). However, another more conditional form of Pearl causal inference attribution statements can be formulated with an imposed-global warming hindcast attribution method (Bercos-Hickey & Patricola, 2021; Bercos-Hickey et al., 2021; Patricola & Wehner, 2018; Patricola et al., 2022; Schär et al., 1996; Wehner et al., 2019). In this approach, ensembles of regional climate model (ReGCM) simulations are performed with historical initial and boundary conditions, referred to as historical or hindcast simulations. These simulations are then compared with simulations performed with counterfactual initial and boundary conditions that have been adjusted by a climate change difference, here referred to as the *deltas*, that takes into account the thermodynamic component of anthropogenic climate change (Section S5 in Supporting Information S1). In this study, the counterfactual experiments include a world without anthropogenic climate change, referred to as natural, as well as worlds with future 21st century warming, referred to as mid-century and late-century. While this approach implies that no attribution statement can be made about the human-induced change in probability of the event, quantitative attribution statements about the human-induced change in the magnitude of the event can be made with this more restricted approach.

In this study, the Weather Research and Forecasting (WRF) model (Skamarock et al., 2008) version 3.8.1 was used to perform hindcast simulations of the PNW heatwave (Section S2 in Supporting Information S1). To understand the impacts of model structural uncertainty, we performed a similar suite of simulations using the International Centre for Theoretical Physics RegCM version 4.9.5 (Giorgi et al., 2012). The WRF hindcast

simulations were initialized on 24 June 2021 00:00 UTC and ran continuously through 4 July 2021 with initial and boundary conditions from the 32 km resolution National Centers for Environmental Prediction North American Regional Reanalysis (NARR). The RegCM hindcast simulations were initialized on 22 June 2021 00:00 UTC and ran continuously through 02 July 2021 with initial and boundary conditions from the Global Forecast System (GFS) version 4 0.5-degree analysis (Section S3 in Supporting Information S1). Ten-member ensembles were performed for each model configuration and the effects of horizontal resolution were explored by configuring the models with grids of 18 and 50 km spacings over the chosen domains (Figure S2 in Supporting Information S1).

To establish the validity of the heatwave simulations, we compare the WRF and RegCM hindcasts with observational and reanalysis data. As discussed in Section S4 in Supporting Information S1, the WRF and RegCM hindcasts capture the omega blocking pattern and elevated temperatures of the PNW heatwave. The two models, however, underestimate the magnitude of the heatwave, likely due to the initial and boundary conditions. The hindcasts of the heatwave event were best represented at 18 km horizontal resolution (Section S4 in Supporting Information S1), and are the basis of the remainder of our analyses.

In addition to the hindcast simulations of the heatwave under current climatic conditions, three ten-member ensembles under counterfactual conditions both cooler and warmer than present were performed using the hindcast attribution method to understand the effects of global warming on the PNW heatwave. Simulations of the event in a cooler "world that might have been" without climate change (here denoted *natural*) were driven by initial and boundary atmospheric conditions altered by the difference between Coupled Model Intercomparison Project Phase 6 (CMIP6) *historical* and *hist-nat* simulations (Danabasoglu, 2019) averaged over the 1995–2014 period (Section S5 and Table S1 in Supporting Information S1). In this study, the multimodel average global average surface temperature of the CMIP6 *hist-nat* simulations is about 0.8°C cooler than the *historical* simulations over this period. Two "worlds that might be" experiments with additional global warming were performed with mid-21st century (2040–2060) and late-21st century (2070–2090) climate conditions under the Shared Socioeconomic Pathway 585 (SSP585) emissions scenario (O'Neill et al., 2016). In this study, the CMIP6 multimodel average global average surface temperature of the former (*mid-century*) is about 1.75°C warmer than the *historical* simulations while the latter (*late-century*) are about 3.8°C warmer. These hindcasts further elucidate the effect of global warming on the PNW heatwave. Lastly, to examine the effects of climate change on soil moisture-temperature feedbacks, natural, mid-, and late-21st century experiments were conducted with the 18 km WRF model by additionally altering soil moisture. A summary of all model experiments is shown in Table S2 in Supporting Information S1.

In the following section, our analyses utilize spatial averages over the region 45–52°N and 124–119°W (Figure S2 in Supporting Information S1). Because WRF and RegCM were run at finer resolution than the CMIP-class models in Philip et al. (2021), we extended the region of interest to the west to be closer to the coast than the WWA region.

4. Changes in PNW Heatwave Temperature

The effects of the current amount of climate change on the PNW heatwave are assessed by comparing the WRF and RegCM simulations in the historical and natural climates. Figure 3 shows the 25 June 25–1 July 2021 time series of Figure 3a the GHCN, NARR, GFS, WRF, and RegCM daily maximum temperature and Figure 3b the WRF and RegCM temperature differences between the climate scenarios and the historical. Contours of the maximum temperature on 28 June, the hottest day of the GHCN station observations (Figure 3a), are shown for the Figures 3c and 3f historical, Figures 3d and 3g historical minus natural, and Figures 3e and 3h late-century minus historical simulations from the 18 km Figures 3c–3e WRF and Figures 3f–3h RegCM. From Figure 3d, the WRF model clearly exhibits warming from the natural to the historical climate except for some cooling at the Oregon coast. From Figure 3g, the RegCM model exhibits a more heterogeneous warming and the cooling is shifted northward to the coast of British Columbia. In our analysis region (Figures 3c and 3f black box), the ensemble average increase in the daily maximum two-meter temperature on 28 June is 0.95°C ± 0.22°C for WRF and 0.66°C ± 0.05°C for RegCM from the natural to the historical, where the confidence intervals are the standard errors. Over the four-day period 27–30 June, during which multiple temperature records were broken, the average increase in daily maximum two-meter temperature is 0.98°C ± 0.40°C for WRF and 0.78°C ± 0.07°C for RegCM from the natural to the historical. The blue lines in Figure 3b reveal that the attributable warming in the WRF model averaged over the region of interest (about 1°C) does not vary much during the heatwave event. The
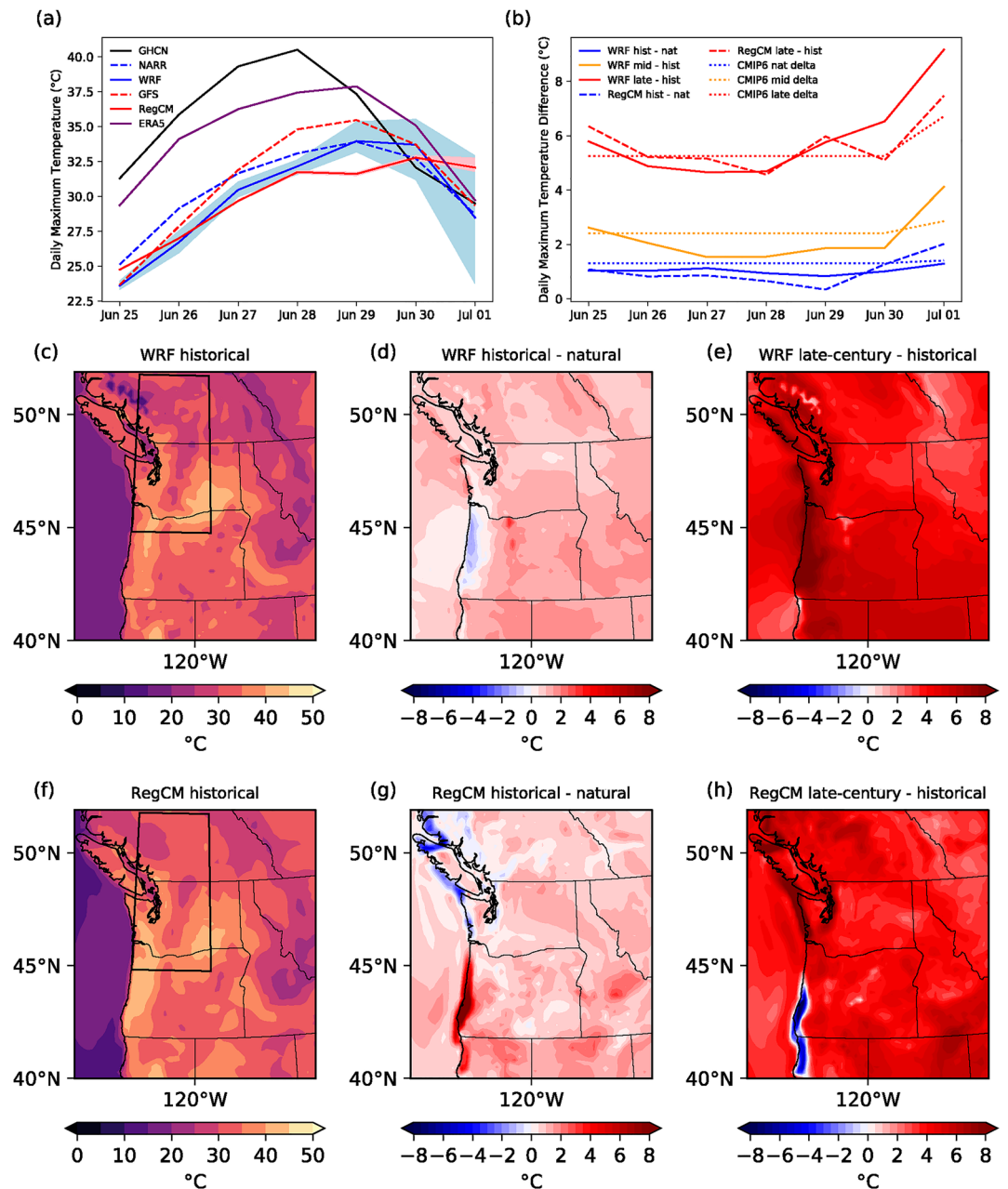
Figure 3. 25 June–1 July 2021 daily maximum temperature (a) from the Global Historical Climatology Network, North American Regional Reanalysis, Global Forecast System, ERA5, and the Weather Research and Forecasting (WRF) and regional climate model (RegCM) historical 18 km ensembles and (b) daily maximum temperature difference between the WRF and RegCM historical and natural, mid-century (WRF only), and late-century ensembles and the Coupled Model Intercomparison Project Phase 6 multi-model surface temperature deltas averaged over the region 45–52°N and 124–119°W. The shading in panel (a) shows the range of values over the WRF and RegCM 10-member ensembles. Ensemble-averaged daily maximum 2 m temperature (°C) on 28 June of the (c and f) historical, (d and g) historical minus natural, and (e and h) late-century minus historical simulations from the 18 km (c–e) WRF with the soil moisture delta and (f–h) RegCM. Black boxes in panels (c and f) are the regions used for spatial averaging, also shown in Figure S2 in Supporting Information S1.

RegCM, which here differs from the WRF model in that soil moisture was not altered in the natural simulations, exhibits a decrease in attributable warming until 28 June and then an increase until 1 July.

Figure 3e shows that the WRF simulated heatwave is warmer over the entire domain under late-century conditions when compared to the historical simulations. Similar warming is also seen in the WRF simulations under

mid-century conditions (not shown). In contrast, Figure 3h shows that while the RegCM model warms over the majority of the region under late-century conditions, cooling is simulated along the coast of southern Oregon and northern California. This coastal cooling in the RegCM late-century simulations is likely due to a complicated interaction between changes in onshore winds and a warmed ocean and is influenced by topography (Figure S10 in Supporting Information S1) and the choice of boundary layer parameterization scheme. In our analysis region (Figures 3c and 3f black box), the average increase in the daily maximum two-meter temperature on 28 June is 1.55°C ± 0.29°C for WRF from the historical to the mid-century, and is 4.68°C ± 0.26°C for WRF and 4.57°C ± 0.04°C for RegCM from the historical to the late-century. During the peak days of the heatwave, the 27–30 June average increase in maximum daily two-meter temperature is 1.71°C ± 0.39°C for WRF from the historical to the mid-century, and is 5.41°C ± 0.41°C for WRF and 5.20°C ± 0.06°C for RegCM from the historical to the late-century.

The red lines in Figure 3b compare the regionally averaged temperature change between the present and late-century under SSP585 forcing conditions. The orange line shows a similar result under mid-century SSP585 forcing conditions. In these warmer simulations, the anthropogenic warming of the PNW heatwave gradually reduces until the hottest days are reached, 29 June 2021. Afterward, the anthropogenic warming increases as the heatwave evolves for both models, lengthening the duration of the heatwave in both the WRF and RegCM simulations. This behavior is also exhibited in the RegCM historical compared to natural simulations (blue dashed line), but is not for WRF, where the regionally averaged anthropogenic warming is relatively constant over the entire duration of the simulation.

To examine the effects of soil moisture-temperature feedback on the PNW heatwave, we performed WRF experiments where, in addition to the other modified fields, we adjusted the soil moisture by a climate change delta. Inclusion of the soil moisture delta causes warmer climates to have drier soil and cooler climates to have wetter soil due to evapotranspiration changes, as can be see in Figure S11 in Supporting Information S1. Figure 4 shows the 28 June 2021 ensemble-averaged maximum two-meter temperature changes from the 18 km WRF Figure 4a natural, Figure 4b mid-century, and Figure 4c late-century experiments including the soil moisture delta minus the experiments without the soil moisture delta. Figure 4d shows the 25 June–1 July time series of the daily maximum temperature in the soil moisture minus no soil moisture experiments. From Figure 4a, the heatwave in the natural climate is cooler across most of the region when the soil moisture delta is included, because of an increase in evapotranspiration cooling from the wetter surface. Thus by also considering that soil conditions are drier now than they were in a cooler past climate, the human effect on the PNW heatwave is slightly larger than in Figure 3a. In our analysis region (Figures 3c and 3f black box), the average daily maximum two-meter temperature in Figure 4a is 0.10°C ± 0.21°C cooler in the natural experiment with the soil moisture delta than it is without. Figures 4b and 4c indicate that the heatwave in the mid- and late-century climates is warmer across almost all of the region when the soil moisture delta is included, reflecting a decrease in evapotranspiration cooling due to less available soil moisture. The average daily maximum two-meter temperature in Figures 4b and 4c is 0.78°C ± 0.34°C and 0.90°C ± 0.28°C warmer in the mid- and late-century experiments with the soil moisture delta, respectively.

The blue line in Figure 4d reveals that the effects of soil moisture on the natural simulations remains relatively constant throughout the duration of the heatwave. In contrast, the future climate simulations (Figure 4d orange and red lines) exhibit a temporally dependent enhancement of the effects of the soil moisture delta as the heatwave progresses. Roughly following the simulated temperature itself (Figure 3a), the effect of decreased soil moisture peaks at about 1.0°C and 1.2°C warmer in the mid- and late-century experiments, respectively.

5. Conclusions

The 2021 PNW heatwave was a rare and unprecedented compound weather event. An unusual summertime AR interacted with an omega block pattern and preexisting dry soil conditions to shatter century-old temperature records by several degrees Centigrade. While there is little doubt that anthropogenic global warming contributed to the probability and magnitude of the extreme temperatures, the uniqueness of the event precludes quantifying this influence by traditional event attribution methods. In Section 2, we demonstrated that out of sample fitted non-stationary GEV distributions fail to contain many of the observed 2021 observations within the uncertainty estimates of their upper bounds. While including the 2021 temperatures in the GEV fitting procedure extends the upper bounds to include these values in the distribution, these distributions are a poor fit to the rest of the
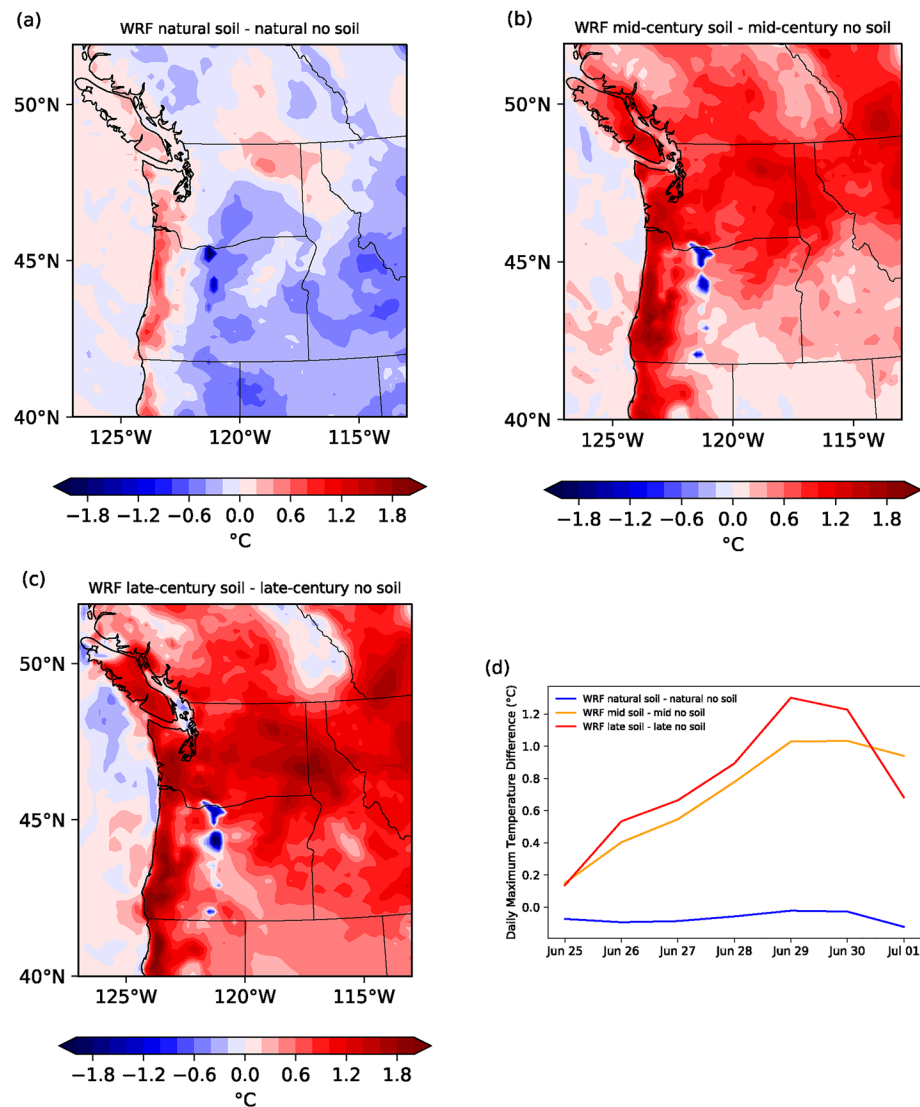
Figure 4. Ensemble-averaged daily maximum 2 m temperature (°C) on 28 June 2021 from the 18 km Weather Research and Forecasting (a) natural, (b) mid-century, and (c) late-century experiments with the soil moisture delta minus the experiments without the soil moisture delta. (d) The 25 June–1 July 2021 daily maximum temperature difference between the experiments with and without the soil moisture delta averaged over the region 45–52°N and 124–119°W.

data. The underlying reason for this failure of traditional statistical methods is that the uniqueness of the 2021 PNW heatwave violates the i.i.d. assumption of GEV theory. We therefore conclude that estimates of the PNW heatwave return times are not accurate and that confidence in GEV-based estimates of the human influence on the change in the probability of the observed extreme temperatures should be low. We further conclude that quantitative changes in event magnitude and frequency from analysis of TXx from CMIP-class models (Philip et al., 2021; Wehner et al., 2018, 2020) are made with low confidence as it is not clear that global climate models adequately simulate the relevant meteorological phenomena of the PNW heatwave even if they simulate extreme temperature anomalies as high as observed (van Oldenborgh et al., 2021; Van Oldenborgh et al., 2022).

In Sections 3 and 4, we present an alternative but more limited attribution of the anthropogenic changes to the PNW heatwave using ensembles of simulations from the regional models WRF and RegCM, where the hindcast attribution method was used to examine the effects of removing anthropogenic warming and additional future warming. We find that the historical model simulations are in agreement with their initial and boundary condition data sets, but that the observed and simulated gridded products are cooler than station observations during the hot portion of the event. Comparison of the historical heatwave with a counterfactual heatwave in a world

without human-induced warming indicates that the anthropogenic temperature increase is about 1°C and relatively constant over the course of the event. In contrast, the heatwave in an SSP585 world with significant future warming would be 5°C warmer, and the anthropogenic influence extends the peak of the heatwave, indicating a future increase in heatwave duration.

These anthropogenic increases in extreme temperatures during the PNW heatwave are slightly less than the lower bound of the synthesis estimate from the World Weather Attribution project but within the lower bounds of the global climate model estimates (Philip et al., 2021). One possible reason for a smaller anthropogenic temperature increase is that severe drought conditions were being experienced in June 2021 in much of the southern portion of our analysis region, thus the evapotranspiration cooling in all of the simulations is low. Despite the additional surface moistening in our cooler counterfactual "world that might have been" simulations, the region remains in drought with a reduced soil moisture influence on air temperature. In Section 4, we examined the effects of soil moisture in the hindcast experiments and found that, at current levels of global warming, this cooling is altered by only about 0.10°C. As precursor soil conditions from the drought are drier than the average conditions used in traditional CMIP-class heatwave attribution statements, this is not unexpected. Even in much warmer late-century conditions, the maximum soil moisture-temperature feedback is 1.2°C out of over 6°C averaged over our analysis region. While it may be that the amplification of the anthropogenic temperature change during heatwaves (Seneviratne et al., 2021) is diminished by pre-existing drought conditions, this is not the case in much warmer future simulations.

This study is limited by the constraints of the hindcast attribution method. Other estimates of the imposed warming could be made by selecting individual CMIP models or other subsets of them. Furthermore, the selection of initial and boundary conditions also affects the limited set of models' ability to reproduce independent observations. However, this study reveals that our understanding of all the physical mechanisms behind this extreme heatwave and their anthropogenic changes is limited and our traditional attribution tools fail for this and other extreme outlier events as pointed out by the great attribution scientist Geert Jan van Oldenborgh in his final paper (Van Oldenborgh et al., 2022). As he had hoped, we indeed can do better and there may be opportunities to remedy this by examining the large coupled and uncoupled model ensembles (Kay et al., 2015; Stone et al., 2019). Presently, however, we do not know with confidence whether the 2021 PNW heatwave and the associated weather patterns will remain an outlier event or is a harbinger of things to come.

Data Availability Statement

WRF and RegCM data are available at https://portal.nersc.gov/archive/home/projects/cascade/www/PNW_Heatwave. Monthly CMIP6 data (variables *hur*, *hus*, *mrsol*, *ps*, *ta*, *ts*, and *zg*) used to create the deltas are available at esgf-node.llnl.gov under the *historical* and *hist-nat* experiments.

References

Baker, M., & Sergio, O. (2021). The Pacific Northwest, built for mild summers, is scorching yet again.

Bercos-Hickey, E., & Patricola, C. M. (2021). Anthropogenic influences on the African easterly jet-African easterly wave system. *Climate Dynamics*, *57*(9–10), 2779–2792. https://doi.org/10.1007/s00382-021-05838-1

Bercos-Hickey, E., Patricola, C. M., & Gallus, W. A. (2021). Anthropogenic influences on Tornadic storms. *Journal of Climate*, *34*(22), 8989–9006. https://doi.org/10.1175/JCLI-D-20-0901.1

Black, E., Blackburn, M., Harrison, G., Hoskins, B., & Methven, J. (2004). Factors contributing to the summer 2003 European heatwave. *Weather*, *59*(8), 217–223. https://doi.org/10.1256/wea.74.04

Campbell, S., Remenyi, T. A., White, C. J., & Johnston, F. H. (2018). Heatwave and health impact research: A global review. *Health & Place*, *53*, 210–218. https://doi.org/10.1016/j.healthplace.2018.08.017

Danabasoglu, G. (2019). *NCAR CESM2 model output prepared for CMIP6 CMIP*. Earth System Grid Federation. https://doi.org/10.22033/ESGF/CMIP6.2185

Diffenbaugh, N. S., & Ashfaq, M. (2010). Intensification of hot extremes in the United States. *Geophysical Research Letters*, *37*(15), L15701. https://doi.org/10.1029/2010GL043888

Di Liberto, T. (2021). *Astounding heat obliterates all-time records across the Pacific Northwest and Western Canada in June 2021*. National Oceanic and Atmospheric Administration. Retrieved from https://www.climate.gov/news-features/event-tracker/astounding-heat-obliterates-all-time-records-across-pacific-northwest

Dole, R., Hoerling, M., Perlwitz, J., Eischeid, J., Pegion, P., Zhang, T., et al. (2011). Was there a basis for anticipating the 2010 Russian heat wave? *Geophysical Research Letters*, *38*(6), L06702. https://doi.org/10.1029/2010GL046582

Ebert-Uphoff, I., & Deng, Y. (2012). Causal discovery for climate research using graphical models. *Journal of Climate*, *25*(17), 5648–5665. https://doi.org/10.1175/JCLI-D-11-00387.1

Fischer, E. M., Sippel, S., & Knutti, R. (2021). Increasing probability of record-shattering climate extremes. *Nature Climate Change*, *11*(8), 689–695. https://doi.org/10.1038/s41558-021-01092-9

Giorgi, F., Coppola, E., Solmon, F., Mariotti, L., Sylla, M., Bi, X., et al. (2012). RegCM4: Model description and preliminary tests over multiple CORDEX domains. *Climate Research*, *52*, 7–29. https://doi.org/10.3354/cr01018

Hannart, A., Pearl, J., Otto, F. E. L., Naveau, P., & Ghil, M. (2016). Causal counterfactual theory for the attribution of weather and climate-related events. *Bulletin of the American Meteorological Society*, *97*(1), 99–110. https://doi.org/10.1175/BAMS-D-14-00034.1

Hersbach, H., Bell, B., Berrisford, P., Hirahara, S., Horányi, A., Muñoz-Sabater, J., et al. (2020). The ERA5 global reanalysis. *Quarterly Journal of the Royal Meteorological Society*, *146*(730), 1999–2049. https://doi.org/10.1002/qj.3803

Horton, D. E., Johnson, N. C., Singh, D., Swain, D. L., Rajaratnam, B., & Diffenbaugh, N. S. (2015). Contribution of changes in atmospheric circulation patterns to extreme temperature trends. *Nature*, *522*(7557), 465–469. https://doi.org/10.1038/nature14550

Kay, J. E., Deser, C., Phillips, A., Mai, A., Hannay, C., Strand, G., et al. (2015). The Community Earth System Model (CESM) large ensemble project: A community resource for studying climate change in the presence of internal climate variability. *Bulletin of the American Meteorological Society*, *96*(8), 1333–1349. https://doi.org/10.1175/BAMS-D-13-00255.1

Lin, H., Mo, R., & Vitart, F. (2022). The 2021 western North American heatwave and its subseasonal predictions. *Geophysical Research Letters*, *49*(6), e2021GL097036. https://doi.org/10.1029/2021GL097036

McEvoy, D., Ahmed, I., & Mullett, J. (2009). The impact of the 2009 heat wave on Melbourne's critical infrastructure. *Local Environment*, *17*(8), 783–796. https://doi.org/10.1080/13549839.2012.678320

McKinnon, K. A., & Simpson, I. R. (2022). How unexpected was the 2021 Pacific Northwest heatwave? *Geophysical Research Letters*, *49*(18), e2022GL100380. https://doi.org/10.1029/2022GL100380

Meehl, G. A., & Tebaldi, C. (2004). More intense, more frequent, and longer lasting heat waves in the 21st century. *Science*, *305*(5686), 994–997. https://doi.org/10.1126/science.1098704

Meehl, G. A., Tebaldi, C., & Adams-Smith, D. (2016). US daily temperature records past, present, and future. *Proceedings of the National Academy of Sciences of the United States of America*, *113*(49), 13977–13982. https://doi.org/10.1073/pnas.1606117113

Min, S.-K., Zhang, X., Zwiers, F., Shiogama, H., Tung, Y.-S., & Wehner, M. (2013). Multimodel detection and attribution of extreme temperature changes. *Journal of Climate*, *26*(19), 7430–7451. https://doi.org/10.1175/JCLI-D-12-00551.1

Miralles, D. G., Teuling, A. J., van Heerwaarden, C. C., & Vilà-Guerau de Arellano, J. (2014). Mega-heatwave temperatures due to combined soil desiccation and atmospheric heat accumulation. *Nature Geoscience*, *7*(5), 345–349. https://doi.org/10.1038/ngeo2141

Mo, R., Lin, H., & Vitart, F. (2022). An anomalous atmospheric river linked to the late June 2021 western North America heatwave. *Communications Earth & Environment*. (in revision). https://doi.org/10.21203/rs.3.rs-1125330/v1

Neal, E., Huang, C. S. Y., & Nakamura, N. (2022). The 2021 Pacific Northwest heat wave and associated blocking: Meteorology and the role of an upstream cyclone as a diabatic source of wave activity. *Geophysical Research Letters*, *49*(8), e2021GL097699. https://doi.org/10.1029/2021GL097699

O'Neill, B. C., Tebaldi, C., Van Vuuren, D. P., Eyring, V., Friedlingstein, P., Hurtt, G., et al. (2016). The scenario Model Intercomparison Project (ScenarioMIP) for CMIP6. *Geoscientific Model Development*, *9*(9), 3461–3482. https://doi.org/10.5194/gmd-9-3461-2016

Patricola, C. M., & Wehner, M. F. (2018). Anthropogenic influences on major tropical cyclone events. *Nature*, *563*(7731), 339–346. https://doi.org/10.1038/s41586-018-0673-2

Patricola, C. M., Wehner, M. F., Bercos-Hickey, E., Maciel, F. V., May, C., Mak, M., et al. (2022). Future changes in extreme precipitation over the San Francisco Bay Area: Dependence on atmospheric river and extratropical cyclone events. *Weather and Climate Extremes*, *36*, 100440. https://doi.org/10.1016/j.wace.2022.100440

Pearl, J. (2009). *Causality*. Cambridge University Press.

Perkins, S. E. (2015). A review on the scientific understanding of heatwaves-their measurement, driving mechanisms, and changes at the global scale. *Atmospheric Research*, *164–165*, 242–267. https://doi.org/10.1016/j.atmosres.2015.05.014

Perkins, S. E., Alexander, L. V., & Nairn, J. R. (2012). Increasing frequency, intensity and duration of observed global heatwaves and warm spells. *Geophysical Research Letters*, *39*(20), L20714. https://doi.org/10.1029/2012GL053361

Perkins-Kirkpatrick, S. E., & Alexander, L. V. (2013). On the measurement of heat waves. *Journal of Climate*, *26*(13), 4500–4517. https://doi.org/10.1175/jcli-d-12-00383.1

Perkins-Kirkpatrick, S. E., & Gibson, P. B. (2017). Changes in regional heatwave characteristics as a function of increasing global temperature. *Scientific Reports*, *7*(1), 12256. https://doi.org/10.1038/s41598-017-12520-2

Philip, S. Y., Kew, S. F., van Oldenborgh, G. J., Anslow, F. S., Seneviratne, S. I., Vautard, R., et al. (2021). Rapid attribution analysis of the extraordinary heatwave on the Pacific coast of the US and Canada June 2021. *Earth System Dynamics Discussions*, *2021*, 1–34. https://doi.org/10.5194/esd-2021-90

Popovich, N., & Choi-Schagrin, W. (2021). Hidden toll of the northwest heat wave: Hundreds of extra deaths.

Power, S. B., & Delage, F. P. D. (2019). Setting and smashing extreme temperature records over the coming century. *Nature Climate Change*, *9*(7), 529–534. https://doi.org/10.1038/s41558-019-0498-5

Rennie, J., Bell, J. E., Kunkel, K. E., Herring, S., Cullen, H., & Abadi, A. M. (2019). Development of a submonthly temperature product to monitor near-real-time climate conditions and assess long-term heat events in the United States. *Journal of Applied Meteorology and Climatology*, *58*(12), 2653–2674. https://doi.org/10.1175/jamc-d-19-0076.1

Rex, D. F. (1950). Blocking action in the middle troposphere and its effect upon regional climate. *Tellus*, *2*(4), 275–301. https://doi.org/10.1111/j.2153-3490.1950.tb00331.x

Risser, M., Collins, W., Wehner, M., O'Brien, T., Paciorek, C., O'Brien, J., et al. (2022). A framework for detection and attribution of regional precipitation change: Application to the United States historical record. *Climate Dynamics*, 1–37. https://doi.org/10.21203/rs.3.rs-785460/v1

Ruffault, J., Curt, T., Moron, V., Trigo, R. M., Mouillot, F., Koutsias, N., et al. (2020). Increased likelihood of heat-induced large wildfires in the Mediterranean Basin. *Scientific Reports*, *10*(1), 13790. https://doi.org/10.1038/s41598-020-70069-z

Schaller, N., Sillmann, J., Anstey, J., Fischer, E. M., Grams, C. M., & Russo, S. (2018). Influence of blocking on northern European and western Russian heatwaves in large climate model ensembles. *Environmental Research Letters*, *13*(5), 054015. https://doi.org/10.1088/1748-9326/aaba55

Schär, C., Frei, C., Lüthi, D., & Davies, H. C. (1996). Surrogate climate-change scenarios for regional climate models. *Geophysical Research Letters*, *23*(6), 669–672. https://doi.org/10.1029/96gl00265

Seneviratne, S. I., Zhang, X., Adnan, M., Badi, W., Dereczynski, C., Di Luca, A., et al. (2021). Weather and climate extreme events in a changing climate. In *Climate change 2021: The physical science basis. Contribution of working group i to the sixth assessment report of the intergovernmental panel on climate change*. Cambridge University Press.

Skamarock, W. C., Klemp, J. B., Dudhia, J., Gill, D. O., Barker, D. M., Duda, M. G., et al. (2008). *A description of the advanced research WRF version 3*. NCAR Technical Note NCAR/TN-475+STR.

Stone, D. A., Christidis, N., Folland, C., Perkins-Kirkpatrick, S., Perlwitz, J., Shiogama, H., et al. (2019). Experiment design of the international CLIVAR C20C+ detection and attribution project. *Weather and Climate Extremes*, *24*, 100206. https://doi.org/10.1016/j.wace.2019.100206

Stott, P. A., Christidis, N., Otto, F. E. L., Sun, Y., Vanderlinden, J.-P., van Oldenborgh, G. J., et al. (2016). Attribution of extreme weather and climate-related events. *WIREs Climate Change*, *7*(1), 23–41. https://doi.org/10.1002/wcc.380

Sumner, E. J. (1954). A study of blocking in the Atlantic-European of the northern hemisphere. *Quarterly Journal of the Royal Meteorological Society*, *80*(345), 402–416. https://doi.org/10.1002/qj.49708034510

Sun, Q., Miao, C., Hanel, M., Borthwick, A. G. L., Duan, Q., Ji, D., & Li, H. (2019). Global heat stress on health, wildfires, and agricultural crops under different levels of climate warming. *Environment International*, *128*, 125–136. https://doi.org/10.1016/j.envint.2019.04.025

van Oldenborgh, G. J., van der Wiel, K., Kew, S., Philip, S., Otto, F., Vautard, R., et al. (2021). Pathways and pitfalls in extreme event attribution. *Climatic Change*, *166*(1), 13. https://doi.org/10.1007/s10584-021-03071-7

Van Oldenborgh, G. J., Wehner, M. F., Vautard, R., Otto, F. E. L., Seneviratne, S. I., Stott, P. A., et al. (2022). Attributing and projecting heatwaves is hard: We can do better. *Earth's Future*, *10*(6), e2021EF002271. https://doi.org/10.1029/2021EF002271

Vogel, M. M., Zscheischler, J., Fischer, E. M., & Seneviratne, S. I. (2020). Development of future heatwaves for different hazard thresholds. *Journal of Geophysical Research: Atmospheres*, *125*(9), e2019JD032070. https://doi.org/10.1029/2019JD032070

Wehner, M., Gleckler, P., & Lee, J. (2020). Characterization of long period return values of extreme daily temperature and precipitation in the CMIP6 models: Part 1, model evaluation. *Weather and Climate Extremes*, *30*, 100283. https://doi.org/10.1016/j.wace.2020.100283

Wehner, M., Stone, D., Shiogama, H., Wolski, P., Ciavarella, A., Christidis, N., & Krishnan, H. (2018). Early 21st century anthropogenic changes in extremely hot days as simulated by the C20C+ detection and attribution multi-model ensemble. *Weather and Climate Extremes*, *20*, 1–8. https://doi.org/10.1016/j.wace.2018.03.001

Wehner, M., Zarzycki, C., & Patricola, C. (2019). Estimating the human influence on tropical cyclone intensity as the climate changes. In J. Collins & K. J. Walsh (Eds.), *Hurricane risk* (pp. 235–260). Springer.

Woollings, T., Barriopedro, D., Methven, J., Son, S.-W., Martius, O., Harvey, B., et al. (2018). Blocking and its response to climate change. *Current Climate Change Reports*, *4*(3), 287–300. https://doi.org/10.1007/s40641-018-0108-z

Wuebbles, D., Meehl, G., Hayhoe, K., Karl, T. R., Kunkel, K., Santer, B., et al. (2014). CMIP5 climate model analyses: Climate extremes in the United States. *Bulletin of the American Meteorological Society*, *95*(4), 571–583. https://doi.org/10.1175/bams-d-12-00172.1

References From the Supporting Information

Berner, J., Ha, S.-Y., Hacker, J. P., Fournier, A., & Snyder, C. (2011). Model uncertainty in a mesoscale ensemble prediction system: Stochastic versus multiphysics representations. *Monthly Weather Review*, *139*(6), 1972–1995. https://doi.org/10.1175/2010mwr3595.1

Chen, F., & Dudhia, J. (2001). Coupling an advanced land surface-hydrology model with the Penn State-NCAR MM5 modeling system. Part I: Model implementation and sensitivity. *Monthly Weather Review*, *129*(4), 569–585. https://doi.org/10.1175/1520-0493(2001)129<0569:caalsh>2.0.co;2

Dickinson, R. E., Henderson-Sellers, A., Kennedy, P. J., & Wilson, M. F. (1993). Biosphere atmosphere transfer scheme (BATS) version le as coupled for Community Climate Model. NCAR/TN-378+SR(August). *NCAR Tech. Note*, *77*. https://doi.org/10.1029/2009JD012049

Emanuel, K. A. (1991). A scheme for representing cumulus convection in large-scale models. *Journal of the Atmospheric Sciences*, *48*(21), 2313–2329. https://doi.org/10.1175/1520-0469(1991)048<2313:ASFRCC>2.0.CO;2

Emanuel, K. A., & Živković-Rothman, M. (1999). Development and evaluation of a convection scheme for use in climate models. *Journal of the Atmospheric Sciences*, *56*(11), 1766–1782. https://doi.org/10.1175/1520-0469(1999)056<1766:DAEOAC>2.0.CO;2

Etminan, M., Myhre, G., Highwood, E., & Shine, K. (2016). Radiative forcing of carbon dioxide, methane, and nitrous oxide: A significant revision of the methane radiative forcing. *Geophysical Research Letters*, *43*(24), 12–614. https://doi.org/10.1002/2016gl071930

Eyring, V., Bony, S., Meehl, G. A., Senior, C. A., Stevens, B., Stouffer, R. J., & Taylor, K. E. (2016). Overview of the Coupled Model Inter-comparison Project Phase 6 (CMIP6) experimental design and organization. *Geoscientific Model Development*, *9*(5), 1937–1958. https://doi.org/10.5194/gmd-9-1937-2016

Grell, G. A., & Freitas, S. R. (2014). A scale and aerosol aware stochastic convective parameterization for weather and air quality modeling. *Atmospheric Chemistry and Physics*, *14*(10), 5233–5250. https://doi.org/10.5194/acp-14-5233-2014

Grenier, H., & Bretherton, C. S. (2001). A moist PBL parameterization for large-scale models and its application to subtropical cloud-topped marine boundary layers. *Monthly Weather Review*, *129*(3), 357–377. https://doi.org/10.1175/1520-0493(2001)129<0357:AMPPFL>2.0.CO;2

Hodnebrog, Ø., Etminan, M., Fuglestvedt, J., Marston, G., Myhre, G., Nielsen, C., et al. (2013). Global warming potentials and radiative efficiencies of halocarbons and related compounds: A comprehensive review. *Reviews of Geophysics*, *51*(2), 300–378. https://doi.org/10.1002/rog.20013

Hong, S.-Y., & Lim, J.-O. J. (2006). The WRF single-moment 6-class microphysics scheme (WSM6). *Journal of the Korean Meteorological Society*, *42*(2), 129–151.

Hong, S.-Y., & Pan, H.-L. (1996). Nonlocal boundary layer vertical diffusion in a medium-range forecast model. *Monthly Weather Review*, *124*(10), 2322–2339. https://doi.org/10.1175/1520-0493(1996)124<2322:nblvdi>2.0.co;2

Iacono, M. J., Delamere, J. S., Mlawer, E. J., Shephard, M. W., Clough, S. A., & Collins, W. D. (2008). Radiative forcing by long-lived greenhouse gases: Calculations with the AER radiative transfer models. *Journal of Geophysical Research*, *113*(D13), D13103. https://doi.org/10.1029/2008jd009944

Kiehl, J., Hack, J., Bonan, G., Boville, B., Briegleb, B., Williamson, D., & Rasch, P. (1996). Description of the NCAR community climate model (CCM3). *NCAR Tech. Note*, *152*. https://doi.org/10.5065/D6FF3Q99

Meinshausen, M., & Nicholls, Z. R. J. (2018). *Uom-remind-magpie-ssp585-1-2-0: Remind-magpie-ssp585 ghg concentrations*. Earth System Grid Federation. https://doi.org/10.22033/ESGF/input4MIPs.2349

Meinshausen, M., & Vogel, E. (2016). *input4mips.uom.ghgconcentrations.cmip.uom-cmip-1-2-0*. Earth System Grid Federation. https://doi.org/10.22033/ESGF/input4MIPs.1118

O'Brien, T. A., Chuang, P. Y., Sloan, L. C., Faloona, I. C., & Rossiter, D. L. (2012). Coupling a new turbulence parametrization to RegCM adds realistic stratocumulus clouds. *Geoscientific Model Development*, *5*(4), 989–1008. https://doi.org/10.5194/gmd-5-989-2012

O'Brien, T. A., Sloan, L. C., & Snyder, M. A. (2011). Can ensembles of regional climate model simulations improve results from sensitivity studies? *Climate Dynamics*, *37*(5–6), 1111–1118. https://doi.org/10.1007/s00382-010-0900-5

Risser, M., Wehner, M., O'Brien, J., Patricola, C., O'Brien, T., Collins, W., et al. (2021). Quantifying the influence of natural climate variability on in situ measurements of seasonal total and extreme daily precipitation. *Climate Dynamics*, *56*(9–10), 3205–3230. https://doi.org/10.1007/s00382-021-05638-7

Shutts, G. (2005). A kinetic energy backscatter algorithm for use in ensemble prediction systems. *Quarterly Journal of the Royal Meteorological Society*, *131*(612), 3079–3102. https://doi.org/10.1256/qj.04.106

Zhang, L., & Shaby, B. A. (2022). Reference priors for the generalized extreme value distribution. *Statistica Sinica*. https://doi.org/10.5705/ss.202021.0258